1

Formulating Geodynamic Model Problems: Three Case Studies

An ideal geodynamic model respects two distinct criteria: it is sufficiently simple that the essential physics it embodies can be easily understood, yet sufficiently complex and realistic that it can be used to draw conclusions about the earth. It is seldom easy to satisfy both criteria together, and so most geodynamicists tend to emphasize one or the other, according to temperament and education.

However, there is a way to overcome this dilemma: to investigate not just a single model, but rather a hierarchical series of models of gradually increasing complexity and realism. Such an investigation – whether carried out by one individual or by many – is a cumulative one in which the initial study of highly simplified models provides the physical understanding required to guide the formulation and investigation of more complex models. In many cases, the simpler models in such a series can be solved analytically, whereas the subsequent more realistic models require numerical or experimental approaches. To illustrate how the hierarchical approach works in practice, I have chosen three exemplary geodynamic phenomena as case studies: heat transfer from magma diapirs, subduction and the interaction of mantle plumes with the lithosphere. The following discussions emphasize models at the simpler end of the spectrum that are amenable to analytic methods and omit mathematical detail to keep the focus on the conceptual structure of the hierarchical approach.

1.1 Heat Transfer from Mantle Diapirs

Our first example is the ascent of a hot blob or diapir of magma through the lithosphere, a possible mechanism for the formation of island-arc volcanoes (Marsh and Carmichael, 1974; Marsh, 1978). The goal of this model is to determine how far the diapir can move through the colder surrounding material before losing so much of its excess heat that it solidifies. Figure 1.1 illustrates a series of model problems that can be used to investigate this question.

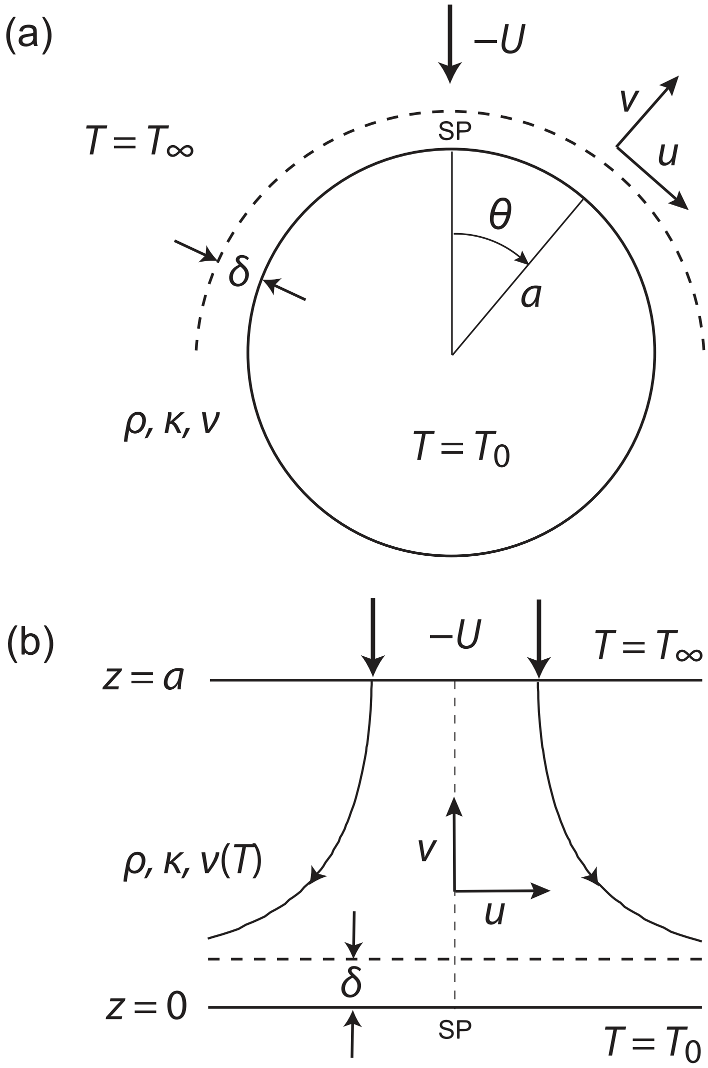

Figure 1.1 Models for the heat transfer from an ascending magma diapir (§ 1.1). (a) Original model in spherical geometry. A spherical diapir of radius a and constant temperature T_0 ascends in an infinite fluid with density ρ, kinematic viscosity ν, thermal diffusivity κ and temperature T_∞ far from the diapir. The viscosity of the fluid inside the diapir is supposed $\ll \nu$. The figure is drawn in the reference frame of the diapir, so that the fluid far from it moves downward with a constant speed $-U$. The colatitude measured from the leading stagnation point (SP) is θ, and the components of the velocity in the colatitudinal and radial directions are u and v, respectively. In the limit $Ua/\kappa \gg 1$, temperature variations in the hemisphere $\theta \leq \pi/2$ are confined to a BL of thickness $\delta \ll a$. The viscosity ν may be constant (Marsh, 1978) or temperature-dependent (Morris, 1982). (b) Stagnation flow model of Morris (1982). The surface of the hot sphere is replaced by the plane $z = 0$, and the far-field streaming velocity $-U$ is imposed as a boundary condition at $z = a$.

Probably the simplest model that still retains much of the essential physics (Marsh, 1978) can be formulated by assuming that (1) the diapir is spherical and has a constant radius; (2) the diapir's interior temperature is uniform and (3) does not vary with time; (4) the ascent speed and (5) the temperature of the lithosphere far from the diapir are constants; (6) the lithosphere is a uniform viscous fluid with constant physical properties and (7) the viscosity of the diapir is much less than that of the lithosphere. The result is the model shown in Figure 1.1a, in which an effectively inviscid fluid sphere with radius a and temperature T_0 ascends at constant speed U through a fluid with constant density ρ, thermal diffusivity κ, kinematic viscosity ν and constant temperature $T = T_\infty \equiv T_0 - \Delta T$ far from the sphere. An analytical solution for the rate of heat transfer q from the diapir (§ 6.2.2) can now be obtained if one makes the additional (and realistic) assumption (8) that the Péclet number $Pe \equiv Ua/\kappa \gg 1$, in which case the temperature variations around the leading hemisphere of the diapir are confined to a thin boundary layer (BL) of thickness $\delta \ll a$ (Figure 1.1a). One thereby finds (see § 2.3 for the derivation)

$$q \sim k_c a \Delta T Pe^{1/2}, \tag{1.1}$$

where k_c is the thermal conductivity.

While the model just described provides a first estimate of how the heat transfer scales with the ascent speed and the radius and excess temperature of the diapir, it is far too simple for direct application to Earth. A more realistic model can be obtained by relaxing assumptions (3) and (5), allowing the temperatures of the diapir and the ambient lithosphere to vary with time. If these variations are slow enough, the heat transfer at each instant will be described by a law of the form (1.1), but with a time-dependent excess temperature $\Delta T(t)$. A model of this type was proposed by Marsh (1978), who obtained a solution in the form of a convolution integral for the evolving temperature of a diapir ascending through a lithosphere with a prescribed far-field temperature $T_{\text{lith}}(t)$.

A different extension of the simple model of Figure 1.1a, also suggested by Marsh (1978), begins from the observation that the viscosity of mantle materials decreases strongly with increasing temperature. A hot diapir will therefore be surrounded by a thin BL of softened lithosphere, which will act as a lubricant and increase the diapir's ascent speed. The effectiveness of this mechanism depends on whether the BL is thick enough and/or has a viscosity low enough, to carry a substantial fraction of the volume flux $\sim \pi a^2 U$ that the sphere must displace in order to move. Formally, this model is obtained by replacing the constant viscosity ν in Figure 1.1a by one that depends exponentially on temperature as $\nu = \nu_0 \exp(-T/\Delta T_r)$, where ΔT_r is a rheological temperature scale.

While this new variable-viscosity model is more realistic and dynamically richer than the original model, its spherical geometry makes an analytical solution difficult. However, closer examination reveals that the spherical geometry is not in fact essential: all that matters is that the flow outside the softened BL varies over a characteristic length scale a that greatly exceeds the BL thickness. This recognition led Morris (1982) to study a simpler model in which the flow around the sphere is replaced by a stagnation flow between two planar boundaries $z = 0$ and $z = a$ (Figure 1.1b). The model equations now admit 1-D solutions $T = T(z)$ and $v = v(z)$ for the temperature and the vertical velocity, respectively, which can be determined using the method of matched asymptotic expansions (§ 6.3) in the limit of large viscosity contrast $\Delta T/\Delta T_{\mathrm{r}} \gg 1$ (Morris, 1982). Because the general scaling relationships revealed by the 1-D solution apply equally well to the original spherical geometry, they can be exploited to simplify the governing equations in spherical coordinates, which can then be solved analytically for certain limiting cases (Morris, 1982; Ansari and Morris, 1985). Further discussion of these problems will be found in § 6.5.2.

1.2 Subduction

Our second example is the subduction of oceanic lithosphere. Faced with the task of devising the simplest possible model for subduction, it makes sense to begin with a purely kinematic approach in which flow is driven by imposed boundary velocities. A minimal list of parameters for such a model comprises a parameter to specify the overall geometry and a velocity to characterize the motion of the slab and the oceanic plate. Figure 1.2a shows an influential model of this type proposed by McKenzie (1969). This 'corner flow' model comprises two wedge-shaped regions containing fluid with a constant viscosity, bounded by rigid surfaces that meet at a corner. The dip of the surface representing the subducting slab is α. The slab and the oceanic plate move away from and towards the corner, respectively, with speed U_0. The overriding plate is motionless. The lines with arrows are typical streamlines for the flow in the two wedges.

An unrealistic aspect of the Newtonian corner flow model is that the stress in the fluid has a nonintegrable singularity $\propto r^{-1}$ at the corner, implying that an infinite force is required to drive subduction. This can be remedied by extending the model to non-Newtonian shear-thinning fluids in which the viscosity decreases with increasing stress. Fenner (1975) showed that corner flows with non-Newtonian rheology can be determined analytically in certain cases. Subsequently, Tovish et al. (1978) extended Fenner's results to the subduction geometry of Figure 1.2a. While the stress is still singular at the corner, the singularity is now integrable. Solutions for non-Newtonian corner flows are derived in § 4.3.3.

Despite their simplicity, corner flow models have been widely used in geodynamic studies where an analytical expression for the subduction-induced mantle

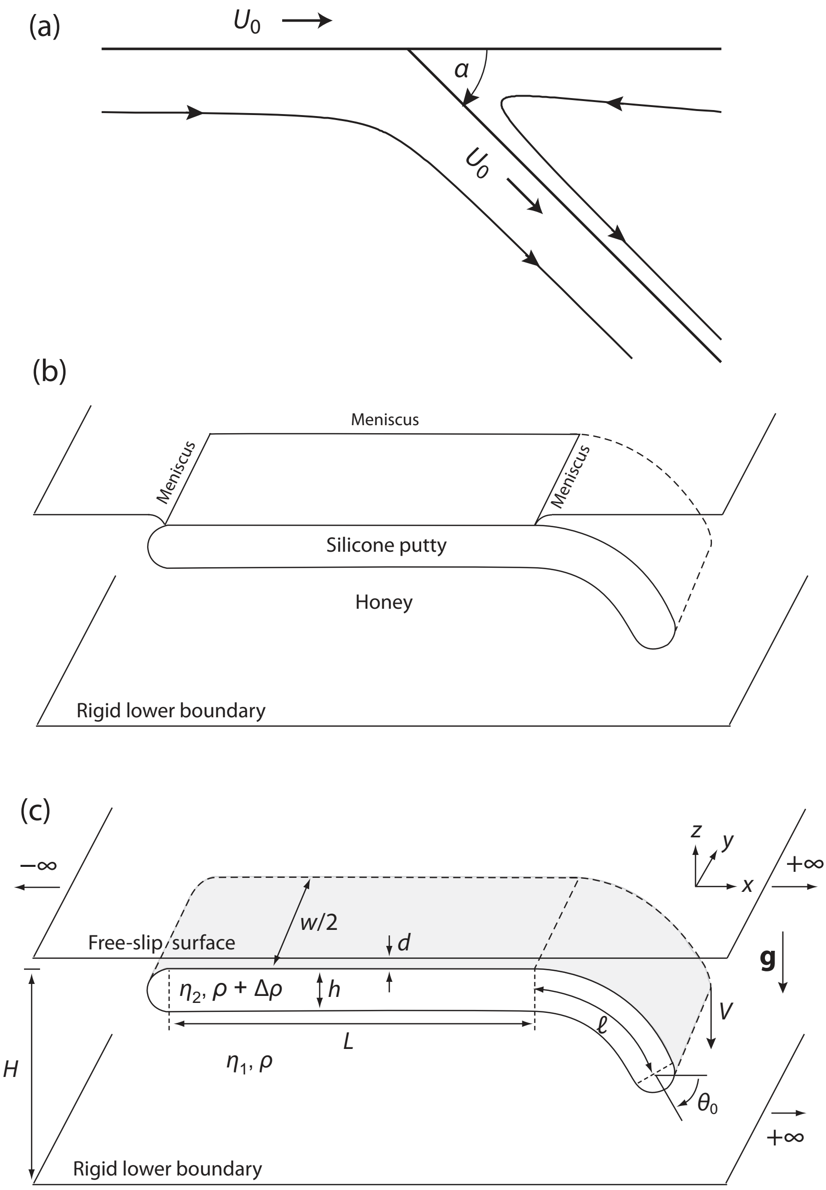

Figure 1.2 Models for the subduction of oceanic lithosphere (§ 1.2). (a) Kinematic corner flow model of McKenzie (1969). (b) Vertical cutaway view of the laboratory configuration studied by Bellahsen et al. (2005). Only the portion of the sheet behind the vertical symmetry plane is shown. The flat portion of the sheet is prevented from sinking by surface tension between the honey and the air acting across a meniscus. (c) Vertical cutaway view of the three-dimensional model of Li and Ribe (2012). Sinking of the flat portion of the sheet is prevented by the presence of a lubrication layer of thickness d between the sheet and the upper free-slip surface.

flow is needed. Nevertheless, they have a number of obvious shortcomings, including their two-dimensionality, the oversimplified geometry of the slab, the stress singularity at the corner and the neglect of the driving buoyancy force and of the viscous force that resists the bending of the plate. The decisive step forward that overcame all these shortcomings was taken in the context of laboratory experiments, using the setup shown schematically in Figure 1.2b (Bellahsen et al., 2005). Earth's upper mantle is represented by a layer of honey $\approx$ 11 cm thick in a transparent tank, and the plate is represented by a thin ($\approx$ 1 cm) sheet of denser silicone putty. The sheet is initially placed flat on top of the honey, where it is prevented from sinking by the surface tension between the honey and the air acting across a meniscus. The experiment is launched by pushing one edge of the sheet down into the honey and letting it subduct freely.

Inspired by these experiments, Li and Ribe (2012) proposed a model (Figure 1.2c) in which surface tension is replaced by a thin lubrication layer of mantle fluid above the sheet. Lubrication theory (§ 7.1) states that the normal stress in the thin layer greatly exceeds the tangential stress. Accordingly, the lubrication layer serves the same purpose as surface tension, which is to prevent the flat part of the sheet from sinking while allowing it to move sideways freely in response to the pull of the slab. However, the advantage of the lubrication layer from a theoretical point of view is that it removes the three-phase (air + honey + putty) contact line. The model then becomes amenable to solution by the semi-analytical boundary-element method (§ 4.6.4). The model of Figure 1.2c will be discussed in more detail in § 8.2.

1.3 Plume–Lithosphere Interaction

Plume–lithosphere interaction refers to the processes that occur after a rising mantle plume impinges on the base of the lithosphere. Because the plume fluid is buoyant relative to its surroundings, it will spread beneath the lithosphere, eventually forming a shallow pool whose lateral dimensions greatly exceed its thickness.

Figure 1.3 shows a series of fluid dynamical models that have been used to study plume–lithosphere interaction, beginning with the kinematic model of Sleep (1987) (Figure 1.3a). Sleep's insight was that the flow associated with a plume rising beneath a moving plate can be regarded as the sum of two parts: a (horizontal) radial flow representing buoyant plume fluid emanating from a steady localized source at the top of the plume conduit and an ambient mantle wind in the direction of the plate motion. Fluid from the source can travel only a finite distance upstream against the wind before being blown back downstream again, leading to the formation of a stagnation point (labelled SP in Figure 1.3a) at which the wind speed just equals the speed of radial outflow from the source. The stagnation streamline that passes through this point (heavy line in Figure 1.3a) divides the (x, y) plane into an inner

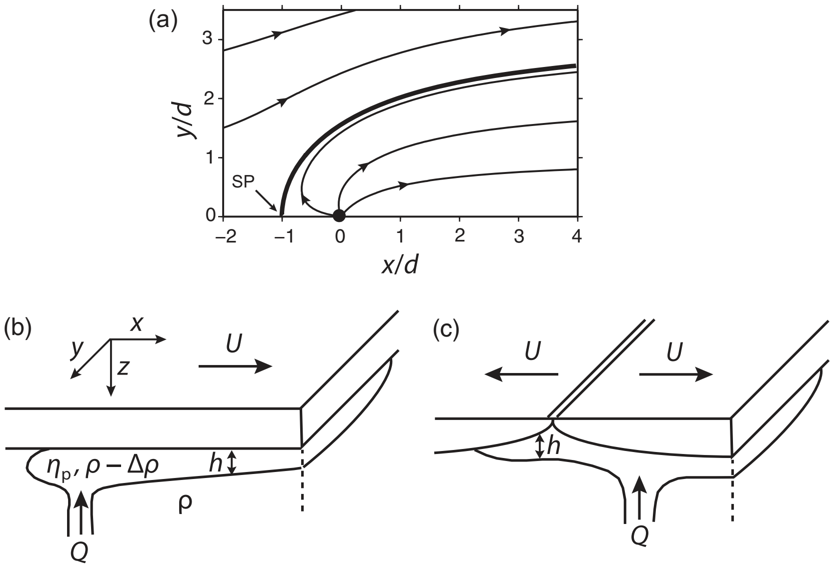

Figure 1.3 Models for plume–lithosphere interaction (§ 1.3). (a) Steady streamlines for the 2-D kinematic model of Sleep (1987). The source is indicated by the black circle, the heavy solid line is the stagnation streamline and d is the distance between the source and the stagnation point SP. (b) Spreading of a pool of buoyant plume fluid supplied at a volumetric rate Q beneath a rigid lithosphere moving at speed U relative to the plume stem (Olson, 1990). The plume fluid has viscosity η_p and density $\rho - \Delta\rho$, where ρ is the density of the ambient mantle. (c) Same as (b), but beneath two plates separated by a spreading ridge with half-spreading rate U (Ribe et al., 1995).

region containing fluid from the source and an outer region containing fluid brought in from upstream by the wind. The stagnation streamline resembles the shape of the topographic swell around the Hawaiian Island chain (Richards et al., 1988).

While the model of Sleep (1987) nicely illustrates the kinematics of plume–plate interaction, it neglects the (driving) buoyancy force and (resisting) viscous force that control the spreading of the plume pool. We now seek the simplest possible model that embodies these dynamics. We first replace the continuous variation of fluid properties by a two-fluid structure, comprising a plume-fed pool with thickness $h(x, y)$, viscosity η_p and density $\rho - \Delta\rho$ spreading in an ambient fluid with viscosity η_m and density ρ. We suppose that the plume stem supplies fluid at a constant volumetric flux Q, at a point (the hotspot) that is fixed relative to a plate moving at a constant speed U. Finally, we assume that $\eta_\mathrm{m}/\eta_\mathrm{p}$, while large, is nevertheless small enough that the resistance of the ambient mantle to the spreading of the pool can be neglected. The result is the 'refracted plume' model of Olson (1990) (Figure 1.3b). Olson's model is in essence a dynamically self-consistent extension of the kinematic model of Sleep (1987). The refracted plume model can be generalized still further while retaining its analytical character by allowing the plume material to have a more realistic non-Newtonian (shear-thinning) rheology (Asaadi et al., 2011).

As a final illustration, Figure 1.3c shows a further extension of the refracted plume model in which the uniform plate is replaced by two plates separated by a spreading ridge. Despite the increased complexity of this plume-ridge interaction model, some analytical results can still be obtained by scaling analysis (Ribe et al., 1995). Plume–plate and plume–ridge interaction models are discussed in more detail in § 7.2.